Journal of Coordination Chemistry

ISSN: 0095-8972 (Print) 1029-0389 (Online) Journal homepage: www.tandfonline.com/journals/gcoo20

The role of 8-quinolinyl moieties in tuning the reactivity of palladium(II) complexes: a kinetic and mechanistic study

Daniel O. Onunga, Deogratius Jaganyi & Allen Mambanda

To cite this article: Daniel O. Onunga, Deogratius Jaganyi & Allen Mambanda (2019) The role of 8-quinolinyl moieties in tuning the reactivity of palladium(II) complexes: a kinetic and mechanistic study, Journal of Coordination Chemistry, 72:3, 499-515, DOI: 10.1080/00958972.2019.1573994

To link to this article: https://doi.org/10.1080/00958972.2019.1573994

JOURNAL OF COORDINATION CHEMISTRY
2019, VOL. 72, NO. 3, 499–515
https://doi.org/10.1080/00958972.2019.1573994

Taylor & Francis
Taylor & Francis Group

The role of 8-quinolinyl moieties in tuning the reactivity of palladium(II) complexes: a kinetic and mechanistic study

Daniel O. Onunga[a], Deogratius Jaganyi[b,c] and Allen Mambanda[a]

[a]School of Chemistry and Physics, University of KwaZulu-Natal, Pietermaritzburg, South Africa;
[b]School of Science, College of Science and Technology, University of Rwanda, Kigali, Rwanda;
[c]Department of Chemistry, Faculty of Applied Sciences, Durban University of Technology, Durban, South Africa

ABSTRACT

The rate and mechanism of chloride substitution from Pd(II) complexes, chlorobis-(2-pyridylmethyl)aminepalladium(II), **1**, chloro-8-[(2-pyridylmethyl)amino]quinolinepalladium(II), **2**, chloro-N-(2-pyridinylmethylene)-8-quinolinaminepalladium(II), **3**, and chlorobis(8-quinolinyl)aminepalladium(II), **4**, are reported. The labile chloride was substituted from the complexes by thiourea nucleophiles *viz*, thiourea (Tu), N,N′-dimethylthiourea (Dmtu) and N,N,N′,N′-tetramethylthiourea (Tmtu). The reactions were monitored under *pseudo*-first-order conditions in methanol using stopped-flow spectrophotometry as a function of concentration and temperature. All the reactions obeyed the rate law $k_{obs} = k_2$[Nu] following the order **1** > **3** > **2** > **4** with **4** exhibiting the slowest rate of substitution due to the stronger σ-donor effect of 8-quinolyl moiety of the coordinated ligand, which makes the Pd center more electron-rich. This slows the nucleophilic attack by the nucleophiles. The values of the thermodynamic parameters ($\Delta H^{\#}$ and $\Delta S^{\#}$) support an associative substitution mechanism. The trends in the DFT calculated data support the experimentally observed order of the reactivity of the complexes.

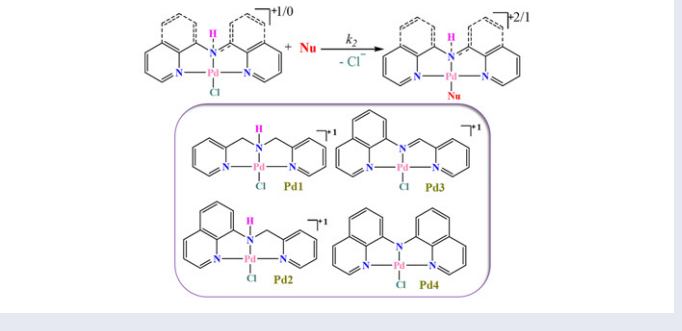

ARTICLE HISTORY
Received 8 November 2018
Accepted 30 December 2018

KEYWORDS
π-Conjugation; electronic effects; quinoline; σ-donation

CONTACT Deogratius Jaganyi deojaganyi@gmail.com

Supplementary data associated with this article can be found in the online version.

1. Introduction

Substitution reactions of square planar Pd(II) and Pt(II) complexes with tridentate N○N○N ligands have attracted attention for over four decades from various investigators [1–5]. The focus has been to tune the reactivity of Pt(II) or Pd(II) complexes with the intention of optimizing it to ensure future complexes with improved antitumor efficacy. Despite a common square planar geometry and similar mechanism of substitution, Pd(II) complexes are 10^2–10^5 more reactive than Pt(II) complexes [3, 6–8] leading to lower antitumor activity of the former complexes. As a result, efforts have been made to design new Pd(II) complexes with reactivity that can be compared to those of Pt(II) complexes so as to minimize their deactivation by biological nucleophiles and thus ultimately improving their antitumor activity. The approach is to use carefully designed spectator ligands with favorable electronic and steric influences to slow the intrinsic reactivity of Pd(II) complexes [9–12].

The interactions of Pt(II) and Pd(II) complexes with sulfur-based biomolecules led to the discovery of the antitumor activity of *cis*-$[PtCl_2(NH_3)_2]$ [13] which can be tracked back to its substitution reaction with nucleophilic biomolecules and has been used for the treatment of several tumors [6, 14, 15]. However, most Pt(II)-based drugs are acutely toxic and some tumor cells develop resistance to their activity [16, 17]. This has prompted interest in designing alternative complexes of d^8 metal ions such as Pd(II) with lower toxicity and improved activity [17]. One of the ways to achieve this is to use a strongly coordinated N-donor and sterically hindered ligands [10, 11]. This ensures stable Pd(II) drugs towards deactivation by biological nucleophiles and thus is able to reach the targeted DNA for therapeutic action. Given the similarity in the coordination chemistry of Pd(II) and Pt(II) complexes, the design of Pd antitumor drugs has followed the same procedures used in developing Pt antitumor drugs [17]. Thus the first step towards tuning the antitumor activity of the Pd(II) complexes is to have a good understanding of the critical factors that influence their reactivity [18].

The rate of the substitution of the leaving chloride or aqua ligand of Pt(II) complexes is influenced by π/σ-donor and π-acceptor characteristics of the spectator ligands [6, 19–26]. For instance, a σ-donating ligand which is coordinated *trans* to the leaving group increases the rate of substitution through its *trans*-influence [25, 27, 28] on the ground state properties of the complex. Strong *cis*- and/or *trans*-π-acceptor ligands, especially those with extended aromatic rings, withdraw electrons from the metal center through π-back bonding as well as π-resonance thereby stabilizing the transition state [20, 21]. As a result, the rate of substitution of the coligand is increased. Moreover, it has been reported that *trans* π-acceptability is weaker than the *cis* π-acceptability while for polypyridyl and related tridentate ligands, the π-acceptability exhibits a multiplicative affect for a conjugated ligand system [20, 21, 24, 29]. However, if the ligand is *cis* coordinated and a strong π/σ-donor, the rate of substitution is decelerated due to increased electron density around the metal center which repels the incoming nucleophiles [25, 27]. This is known as the *cis*-effect [20, 24, 25]. However, ligands with both *cis*-π-acceptor and σ-donating properties can potentially accelerate or decelerate depending on whichever has dominant control on the reactivity since the former increases while the latter decreases the reactivity of the metal center.

Non-antitumor active monofunctional coordination compounds of chloro and aqua Pd(II) and Pt(II) complexes of the N○N○N tridentate ligands such as 2,2′:6′,2″-terpyridine

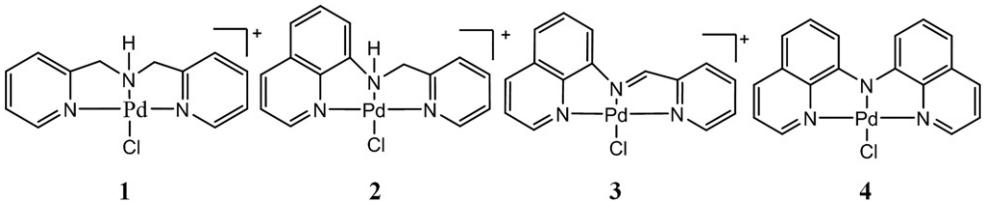

1 2 3 4

Scheme 1. Structures of the Pd(II) complexes under study (where necessary, counter ions omitted for clarity).

(terpy), bis(2-pyridylmethyl)amine (bpma), and diethylenetriamine (dien) [8, 20, 23, 30–34] provided useful model substrates for studying the kinetics and mechanisms of ligand exchange reactions of square-planar complexes [30]. For example, it was shown that the reactivity of these complexes could reduce by five orders of magnitude going from terpy spectator ligand to a dien system. This was because of stepwise reduction of π-back bonding by replacing pyridine donor groups by amine ligands hence reducing electrophilicity of the metal center. Moreover, a systematic increase in π-conjugation around the metal center of terpy framework results in either increase or decrease in the rate of substitution depending on the relative position of the π-extension. The acceleration of the reactivity is due to increase in π-back bonding character caused by favorable overlap of the dπ-orbitals of the metal and the ligands' π*-orbitals [20, 22, 24, 35] while the dampening of reactivity is a result of the net σ-donor effect on the metal center [18, 22, 36].

Given that any structural modification of polypyridyl spectator ligands can produce significant changes on the reactivity of Pd(II) complexes [37–39], derivatives of non-leaving ligands such as bpma can have their lateral pyridines replaced with strong σ-donor quinolinyl rings. This can then be used to slow the high reactivity of the Pd(II) complexes which is necessary to their antitumor activity.

The rate of substitution from Pt(II) complexes with quinolinyl moiety has been reported to be lower than that from analogous complexes with a terpyridyl moiety [18, 22, 36, 40]. However, there is no similar literature on kinetic and mechanistic data aimed at controlling the reactivity of Pd(II) complexes particularly with quinolinyl moieties. With this in mind, the rate and mechanism of substitution from Pd(II) complexes with benzopyridine spectator ligands shown in Scheme 1 was investigated. The substitution reactions were studied using bio-relevant thiourea nucleophiles having varied steric influences. The density function theory (DFT) calculations were performed to provide insight into the observed reactivity trends of the complexes.

2. Experimental

2.1. Materials and methods

All syntheses were done under nitrogen. *RAC*-2,2′-bis(diphenylphosphino)-1,10-binaphthyl (97%), 8-aminoquinoline (98%), 8-bromoquinoline (98%), NaO^{t}Bu (97%), 2-picolylchloride hydrochloride (98%), pyridine-2-carboxyaldehyde (99%), tris(dibenzylideneacetone)-dipalladium(0) (97%), lithium perchlorate (98%), potassium tetrachloropalladate (K_2PdCl_4 99.99%), dichloro-1,5-cyclooctadiene palladium(II) (Pd(COD)Cl_2, 99%), thiourea nucleophiles, and the

ligand, di-(2-picolyl)amine were all purchased from Aldrich and used as received. Solvents were distilled before use and dried through standard procedures [41].

2.2. Synthesis of ligands

The ligands 8-[(2-pyridylmethyl)amino]quinoline and bis(8-quinolinyl)amine (BQA) were synthesized according to the standard published methods [42, 43].

2.2.1. 8-[(2-Pyridylmethyl)amino]quinolone

To a stirring solution of 2-picolylchloride hydrochloride (820 mg, 5 mmol) in water (15 mL) was added aqueous solution (4 mL) of sodium hydroxide (0.01 M) dropwise. Ten minutes later, ethanolic solution (10 mL) of 8-aminoquinoline (288 mg, 2 mmol) was added in portions. To the reaction mixture, 0.01 M aqueous solution of sodium hydroxide (6 mL) was added dropwise under nitrogen and the mixture left to stir for 5 days at room temperature. The crude product was then extracted with chloroform (3×25 mL) and the organic extracts were combined and dried over sodium sulfate. The solvent was removed under reduced pressure to obtain a brown oily gum which was purified by short column chromatography on silica gel using a 4:1 hexane/ethyl acetate. A pure brownish-yellow oil was concentrated from a second elution fraction. Yield (161.0 mg, 34.3%). ^{1}H NMR ($CDCl_3$, 400 MHz, ppm): $\delta = 8.775$ (td, 1H), 8.627 (d, 2H), 8.086 (ddd, 1H), 7.63 (td, 1H), 7.443-7.298 (m, 2H), 7.18 (dd, 1H), 7.077 (dd, 1H), 6.618 (d, 1H), 4.74 (s, 2H). ^{13}C NMR ($CDCl_3$, 100 MHz, ppm): $\delta = 159.3$, 149.3, 147.6, 136.7, 136.3, 127.7, 127.4, 122.0, 121.4, 121.3, 116.3, 114.5, 110.2, 105.6, 49.3. MS ESI$^+$: m/z, $[M + H]^+ = 236$.

2.2.2. Bis(8-quinolinyl)amine (BQA)

Tris(dibenzylideneacetone)dipalladium(0) (22 mg, 0.024 mmol), RAC-2,2′-bis(diphenylphosphino)-1,10-binaphthyl (29.87 mg, 0.048 mmol) and dry toluene (10 mL) were added into a two-necked round-bottomed flask under flow of nitrogen. After allowing the reactants to stir for 5 minutes, 8-bromoquinoline (0.16 mL, 1.2 mmol), 8-aminoquinoline (0.1737 g, 1.2 mmol) and additional dry toluene (20 mL) were added. Subsequently, NaO^tBu (0.1387 g, 1.44 mmol) was added, resulting in a red solution. The reaction mixture was further stirred vigorously for 3 days at 110 °C. The solution was then allowed to cool to room temperature, filtered through a silica plug and extracted with dichloromethane to ensure complete removal of the desired product. Removal of the solvent under reduced pressure yielded a crude red solid. The solid was purified on a short column of silica gel using 4:1 toluene/ethyl acetate as an eluent. An orange solid formed upon evaporation of the solvent. Yield: (293 mg, 89.9%). ^{1}H NMR ($CDCl_3$, 400 MHz, ppm): $\delta = 10.64$ (s, 2H), 8.965 (dd, 2H), 8.23(ddd, 2H), 8.172 (dd, 2H), 7.90 (d, 2H), 7.54-7.459 (m, 4H), 7.343 (d, 2H). ^{13}C NMR ($CDCl_3$, 100 MHz, ppm): $\delta = 147.96$, 139.73, 138.81, 136.93, 129.3, 127.49, 121.70, 118.28, 111.12. Anal. Calcd. for $C_{18}H_{13}N_3$: C, 79.68; H, 4.83; N, 15.49. Found: C, 79.87; H, 4.83; N, 15.21. MS ESI$^+$: m/z, $[M + H]^+ = 272$.

2.3. Synthesis of palladium(II) complexes

The precursor, *trans*-dichlorobis(dimethylsulfide)palladium(II) [44], **1** [45], **2** [40], **3** [46, 47] and **4** [43] were all synthesized according to literature procedures.

2.3.1. Trans-dichlorobis(dimethylsulfide)palladium(II)

In a three-necked round-bottomed flask K_2PdCl_4 (1279.2 mg, 4.12 mmol) was stirred in 100 mL of water until complete dissolution. To the stirring solution dimethyl sulfide (2.25 mL, 0.0615 mol) was added under nitrogen. A pink/yellow precipitate formed immediately. The mixture was refluxed for 1 h during which time all the precipitate dissolved. Microcrystalline orange crystals were formed upon cooling the solution to room temperature and were collected by filtration, washed with cold water and dried under vacuum. NMR analysis confirmed the formation of the complex. Yield: (819.8 mg, 66.0%). ^{1}H NMR ($CDCl_3$, 400 MHz, ppm) $\delta = 2.40$ (s, SMe_2). ^{13}C NMR ($CDCl_3$, 100 MHz, ppm) $\delta = 22.769$ (s, SMe_2). This complex was used as a precursor for the synthesis of **2** and **3**.

2.3.2. Chlorobis(2-pyridylmethyl)aminepalladium(II), 1

To a solution of $Pd(COD)Cl_2$ (156.7 mg, 0.48 mmol) in methanol (20 mL), di-(2-picolyl)-amine (0.1 mL) was added and refluxed at 50 °C for 1 day. The solution mixture was then filtered and the filtrate evaporated to dryness under reduced pressure to give a yellow solid which was washed with THF, diethyl ether and dried under vacuum yielding a yellow powder. Yield: (165.30 mg, 86.3%). ^{1}H NMR (DMSO-d_6, 400 MHz, ppm): $\delta = 8.82$ (dd, 2H), 8.60 (br, s, 1H), 8.23 (ddd, 2H), 7.76 (d, 2H), 7.63 (t, 2H), 4.92 (m, 2H), 4.51 (dd, 2H). ^{13}C NMR (DMSO-d_6, 400 MHz, ppm): $\delta = 167.4$, 149.4, 141.4, 125.7, 123.4, 59.4. Anal. Calcd. for $C_{12}H_{13}N_3PdCl_2 \cdot 1.25H_2O$: C, 36.11; H, 3.91; N, 10.53. Found: C, 36.51; H, 3.80; N, 10.16. TOF MS ESI$^+$: m/z, $[M - Cl]^+ = 342.0280$.

2.3.3. Chloro-8-[(2-pyridylmethyl)amino]quinolinepalladium(II), 2

A solution of 8-[(2-pyridylmethyl)amino]quinoline (155.0 mg, 0.66 mmol) in methanol (5 mL) was added to a refluxing solution of *trans*-$[PdCl_2(SMe_2)_2]$ (199.05 mg, 0.66 mmol) in methanol (15 mL) and allowed to reflux for 12 h. The solution was cooled to room temperature, evaporated to dryness under reduced pressure and washed with acetonitrile, chloroform and diethyl ether and dried under vacuum. Yield: (109.4 mg, 40.2%). ^{1}H NMR (400 MHz, DMSO-d_6, ppm): $\delta = 9.66$ (s, 1H), 8.98 (d, 1H), 8.76 (dd, 1H), 8.65 (dd, 1H), 8.41 (td, 1H), 8.29 (ddd, 1H), 8.04–7.95 (m, 1H), 7.91 (m, 1H), 7.78 (m, 2H), 7.69 (m, 1H), 7.63 (m, 2H). ^{13}C NMR (DMSO-d_6, 100 MHz, ppm): $\delta = 159.8$, 148.7, 147.6, 135.7, 135.3, 128.7, 128.4, 125.0, 122.4, 121.7, 115.3, 113.5, 109.2, 106.6, 51.1. Anal. Calcd. for $C_{15}H_{13}N_3PdCl_2$: C, 43.66; H, 3.18; N, 10.18. Found: C, 43.77; H, 3.35; N 9.79. TOF MS ESI$^+$: m/z, $[M - Cl]^+ = 375.9905$.

2.3.4. Chloro-N-(2-pyridinylmethylene)-8-quinolinaminepalladium(II), 3

A suspension of *trans*-$PdCl_2(SMe_2)_2$ (171.9 mg, 0.57 mmol) in methanol (20 mL) was heated to 50 °C until the complex was completely dissolved. To the solution, a mixture of 8-aminoquinoline (0.082 g, 0.57 mmol) and pyridine-2-carboxyaldehyde (0.05 mL, 0.57 mmol) in methanol (10 mL) was added dropwise. The resulting solution was stirred at room temperature for 3 h

and excess lithium perchlorate (0.35 g, 2.85 mmol) added. A brown solid precipitated from the solution and the reaction mixture was then kept at −10 °C for 1 h. The precipitated product was filtered off, washed with methanol, ethanol and diethyl ether. Yield: (240.9 mg, 89.1%). ^{1}H NMR (400 MHz, DMSO-d_6, ppm): $\delta = 9.62$(s, 1H), 8.94 (dd, 1H), 8.76 (d, 1H), 8.71 (dd, 1H), 8.61 (d, 1H), 8.45 (td, 1H), 8.19 (dd, 1H), 7.99 (d, 1H), 7.62 (ddd, 1H), 7.50 (t, 1H), 7.42 (d, 1H). ^{13}C NMR (100 MHz, DMSO-d_6, ppm): $\delta = 166.9$, 156.9, 149.0, 150.8, 149.6, 148.8, 147.5, 144.5, 141.4, 140.1, 129.6, 129.1, 126.8, 122.9, 122.1, 120.3. Anal. Calcd. for $C_{15}H_{11}N_3PdCl_2O_4$: C, 37.96; H, 2.34; N 8.85. Found: C, 38.28; H, 2.41; N, 9.19. TOF MS ESI$^+$: m/z, $[M - ClO_4]^+ = 375.9718$.

2.3.5. Chlorobis(8-quinolinyl)aminepalladium(II), 4

To a reaction flask containing (COD)$PdCl_2$ (85.37 mg, 0.3 mmol) dissolved in THF (20 mL) was added a THF solution of 8-[(2-pyridylmethyl)amino]quinoline (81 mg, 0.3 mmol) and triethylamine (70 μL, 0.5 mmol). The vessel was sealed and heated at 95 °C for 48 h. Thereafter the mixture was cooled to room temperature and the excess solvent removed in vacuo, affording a red solid. The solid was dissolved in CH_2Cl_2 (50 mL), filtered through Celite on a sintered-glass frit, and washed with dilute brine solution (3 × 20 mL). The volume was reduced in vacuo and the product precipitated from the solution using hexane. The resulting red microcrystalline solid was washed with petroleum ether (3 × 15 mL) and dried to afford spectroscopically pure product. Yield: (78.5 mg, 63.6%). ^{1}H NMR (400 MHz, $CDCl_3$, ppm): $\delta = 8.99$ (d, 2H), 8.22 (d, 2H), 7.67 (d, 2H), 7.49 (m, 2H), 7.40 (m, 2H), 7.09 (d, 2H). ^{13}C NMR (400 MHz, $CDCl_3$, ppm): $\delta = 149.70$, 149.14, 148.55, 138.97, 131.48, 129.6, 121.48, 115.24, 112.56. Anal. Calcd. for $C_{18}H_{12}N_3PdCl$: C, 52.45; H, 2.93; N, 10.19. Found: C, 52.17; H, 2.92; N, 9.85. TOF MS ESI$^+$: m/z, $[2M + Na]^+ = 846.9298$.

2.4. Physical measurements and instrumentation

NMR spectra were acquired using either Bruker Avance DPX 400 NMR or DPX 500 with a 5-mm BBOZ probe at 30 °C. Mass spectra were recorded on Shimadzu LC-MS 2020 or on a Waters TOF Micro-mass LCT Premier mass spectrometers with electrospray ionization source operated on the positive ion mode. Sampled NMR and mass spectra of the synthesized compounds are presented in figures S1–S15 in the Supporting Information (ESI‡). The purity of the compounds was confirmed by elemental analysis using a Carlo Erba Elemental Analyzer 1106. A Cary 100 Bio UV–Visible spectrophotometer was used to determine a suitable wavelength for monitoring the substitution reaction. An Applied Photophysics SX 20 stopped-flow reaction analyzer coupled to an online data acquisition system was used to measure observed rate constants of the substitution reactions as a function of concentration and temperature. The instrument was thermo-controlled within ±0.1 °C.

2.5. Preparations of kinetic solutions

Palladium(II) complex solutions whose concentration was 2.0×10^{-4} M were prepared in 4% DMF to enhance solubility and topped up with 96% methanol containing 20-mM LiCl [48]. Nucleophile solutions were freshly prepared just before use by dissolving a measured quantity in 20-mM LiCl methanolic solution. LiCl was used to suppress the possibility of any solvolysis [49, 50]. The stock solution of the nucleophiles with

approximately 50-fold excess of the concentration of the complex was serially diluted with the methanolic solution to afford 40-, 30-, 20- and 10-fold in excess of the complex concentrations to maintain *pseudo*-first-order conditions.

2.6. Kinetic analysis

To determine the wavelength at which the kinetic measurements would be monitored, the reaction between the solutions of the complexes and the nucleophiles was followed spectrophotometrically by recording the spectral changes over a range of wavelengths between 800 nm and 200 nm. All reactions were initiated by mixing equal volumes of ligand and complex solutions directly in the stopped-flow instrument. The rate of the chloride substitution from the complexes by the entering nucleophiles was monitored as a function of concentration at 298 K. To determine activation parameters $\Delta H^{\neq}$ and $\Delta S^{\neq}$, the rates of reactions were measured within a range of 20 °C–40 °C with 5 °C intervals for all the substitution reactions. All the *pseudo*-first-order rate constants observed, k_{obs}, were average values computed from 4 to 8 independent runs.

2.7. Computational modeling

To understand how the structural and electronic factors affect the kinetics of the substitution reactions ground state electronic structures of the complexes were optimized using the density functional theory (DFT). The DFT calculations were performed with the Gaussian 09 program suite [51] using the B3LYP (Becke 3-Lee-Yang-Parr) functional method, utilizing LANL2DZ (Los Alamos National Laboratory 2 Double ζ) [52] as the basis set. The influence caused by the bulk solvent was evaluated via single-point computations using the C-PCM (conductor-like polarizable continuum model) [53, 54] in methanol. All the complexes were modeled at a charge of +1 except **4**, which was done at 0 charge in accordance to its neutrality [43, 55] and singlet state. Global electrophilicity index (ω) of the complexes was calculated using literature methods [18, 56, 57].

3. Results

3.1. Computational analysis

DFT calculations were performed to gain insights into structural and electronic factors influencing the reactivity of the modeled Pd(II) complexes. The geometry of the optimized molecular frontier orbitals and the planar structures for the complexes are presented in Table 1, while the geometric data extracted from the DFT calculations are presented in Table 2.

The DFT optimized structures reveal that the HOMO of **1** is contributed by the orbitals of ligand's *trans*-nitrogen, Pd and chloride while those of **2** are mostly centered on the Pd and chloride as well as on the quinoline moiety. However, for **3** and **4**, the HOMOs are entirely distributed in the whole complex. The LUMOs of all the complexes are mainly centered on the ligand's aromatic rings with a small contribution from the Pd d-orbitals. Planarity of the complexes increases with increasing π-conjugation comparing well with their analogous Pt(II) complexes [40].

Table 1. DFT optimized minimum energy structures, HOMO and LUMO frontier molecular orbitals, with respective planarity for Pd(II) complexes at B3LYP/LANL2DZ level of theory (Isovalue = 0.02).

Complex structure	HOMO maps	LUMO maps	Planarity
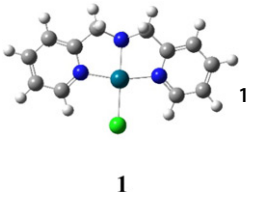 **1**	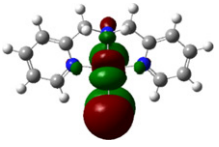	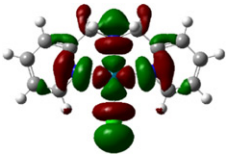	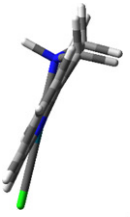
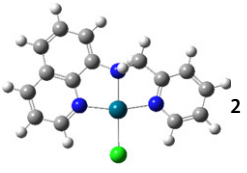 **2**	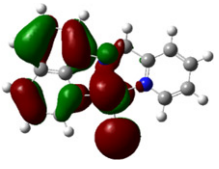	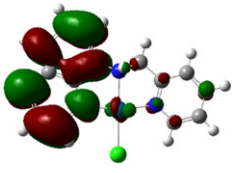	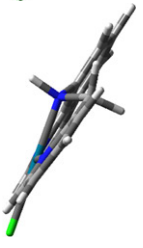
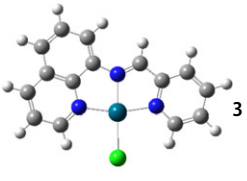 **3**	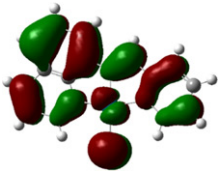	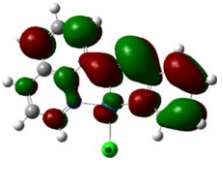	
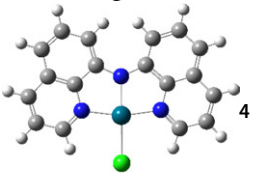 **4**	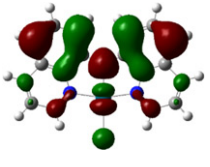	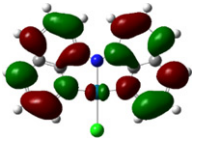	

The data from Table 2 show that the complexes adopt a slightly distorted square-planar geometry with N2–Pd–N3 deviating from 180° by 14.4°–15.5°. The HOMO-LUMO energy gaps decrease in the order **1** > **2** > **3** > **4** which is in accord with their increasing π-conjugation. On stepwise extension of the π-conjugation, the energy levels of the HOMO orbitals are successively raised. This suggests that the σ-donation of electron density towards the Pd(II) [28] increases in the same order.

3.2. Kinetic measurements

The chloride substitution reactions of the Pd(II) complexes with the nucleophiles were investigated as a function of nucleophile concentration and temperature. The reactions were monitored using stopped-flow techniques with a specified wavelength that had been predetermined from the UV–Visible spectra of the reaction between the complex and the nucleophile. The wavelengths used for the substitution reactions ranged

Table 2. Calculated parameters for the Pd(II) complexes.

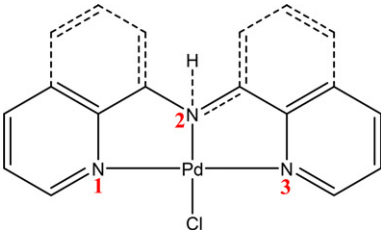

Property	1	2	3	4
NBO charges				
Pd	0.555	0.563	0.577	0.509
N2	−0.632	−0.649	−0.437	−0.570
Cl	−0.518	−0.510	−0.508	−0.566
Electrophilicity index (ω)	6.077	5.696	8.902	4.764
Bond lengths (Å)				
N1–Pd	2.050	2.045	2.046	2.038
N2–Pd	2.059	2.070	2.006	2.003
N3–Pd	2.050	2.049	2.060	2.039
Pd–Cl	2.415	2.411	2.405	2.449
Bond angles (°)				
N2–Pd–Cl	179.77	179.28	179.58	179.98
N1–Pd–N3	165.60	165.49	163.57	165.17
HOMO-LUMO Energy (eV)				
LUMO (eV)	−2.984	−2.809	−3.782	−2.276
HOMO (eV)	−7.545	−7.251	−7.120	–5.241
$\Delta E_{LUMO\text{-}HOMO}$ (eV)	4.561	4.442	3.338	2.965
Dipole moment (*D*)	13.640	12.452	12.789	7.019

between 320 nm and 396 nm depending on the respective complexes and the nucleophiles used as shown in Table S1, Supporting Information (ESI‡). A representative stopped-flow kinetic trace for **3** and Dmtu is shown in Figure 1.

All the kinetic traces from the stopped flow were of excellent fit to a single-exponential decay function suggesting that all the substitution reactions were first-order in both the thiourea nucleophiles and Pd(II) complexes. The observed *pseudo*-first-order rate constant, k_{obs}, was generated from the plots. The second-order rate constants, k_2, for the reactions were obtained from the gradient of a plot of k_{obs} *versus* nucleophile concentration using OriginPro 9.1® software [58]. Straight line plots with zero intercepts were obtained which indicated that the reverse or solvotic pathway was absent or insignificant. A representative plot of k_{obs} *versus* concentration of the nucleophiles of **1** is shown in Figure 2, similar plots for the other complexes are shown in Figures S16–S18, while values of k_{obs} and their respective nucleophile concentrations are presented in Tables S2–S5 in the Supporting Information (ESI‡). From these results, it can be stated that the *pseudo*-first-order dependence upon nucleophile concentration obeys the rate law Equation (1), where the entering thiourea nucleophiles irreversibly displace the leaving chloride ligand from the metal complexes.

$$k_{obs} = k_2 [Nu]. \quad (1)$$

The values of the second-order rate constants, k_2, obtained from the reactions of the complexes are presented in Table 3. Based on the results, the reaction mechanism can therefore be proposed as illustrated in Scheme 2.

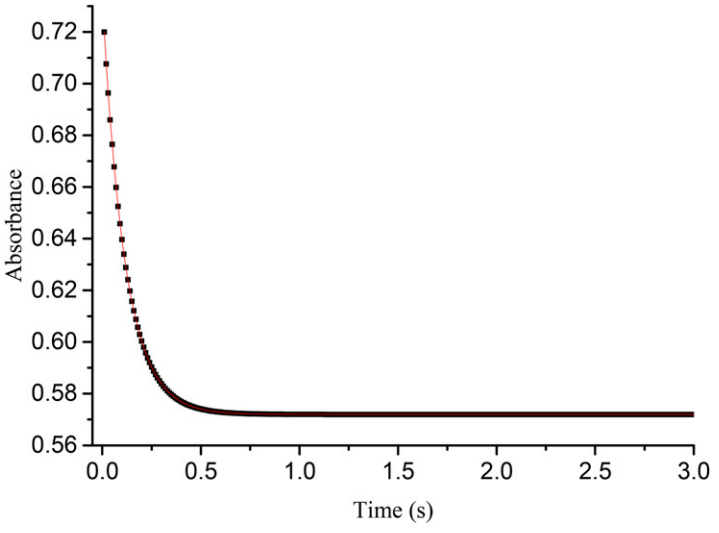

Figure 1. Stopped-flow kinetic trace at 330 nm for the reaction between **3** (2.0×10^{-4} M) and Dmtu (2.0×10^{-3} M) solutions in methanol at 298 K.

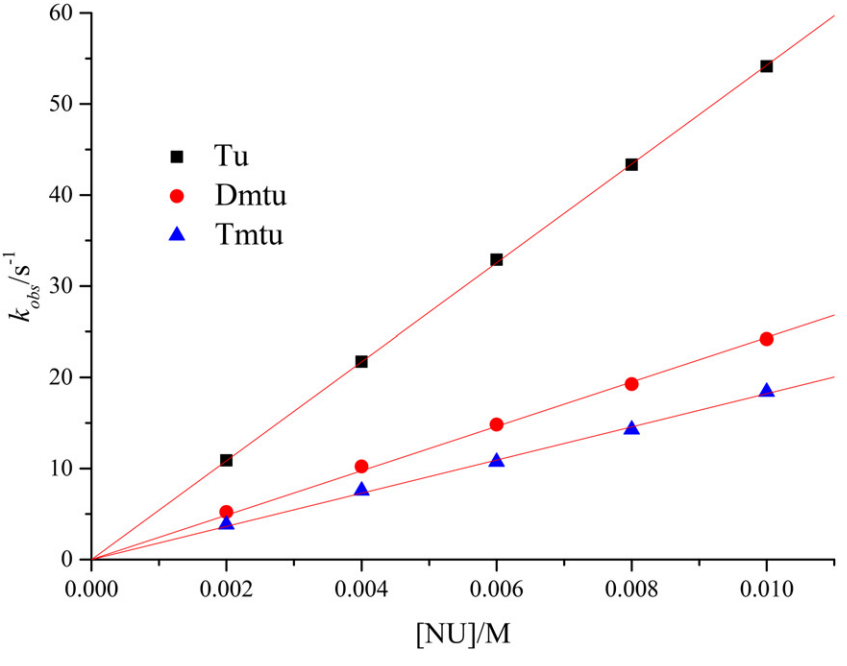

Figure 2. Dependence of the *pseudo*-first-order rate constants (k_{obs}) on the concentration of thiourea nucleophiles for chloride substitution on **1** in methanol, 20 mM LiCl, $T = 298$ K.

From the temperature dependence of k_2, Eyring plots of $\ln\left(\frac{k_2}{T}\right)$ *versus* $\frac{1}{T}$ were constructed. The enthalpy of activation ($\Delta H^{\neq}$) and entropy of activation ($\Delta S^{\neq}$) were calculated from the slopes and y-intercepts, respectively, from the plots according to Eyring Equation (2) [59],

Table 3. Rate constants and thermodynamic parameters for the substitution reactions of Pd(II) complexes by thiourea ligands in methanol, I = 20 mM, LiCl.

Complexes	Nucleophiles	k_2 (M^{-1} s^{-1})	$\Delta H^{\neq}$ (kJ mol^{-1})	$\Delta S^{\neq}$ (JK^{-1} mol^{-1})
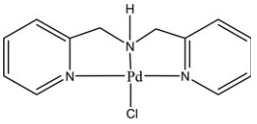	Tu	5427 ± 13	31 ± 1	−70 ± 2
	Dmtu	2438 ± 23	41 ± 1	−43 ± 2
	Tmtu	1822 ± 18	40 ± 1	−43 ± 5
1				
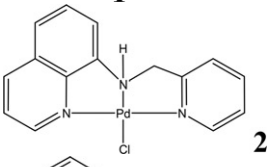	Tu	730 ± 12	36 ± 2	−69 ± 7
	Dmtu	473 ± 13	43 ± 2	−49 ± 7
	Tmtu	332 ± 3	50 ± 2	−28 ± 6
2				
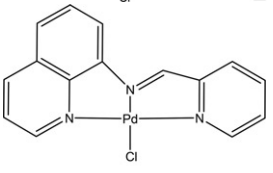	Tu	849 ± 6	45 ± 2	−52 ± 5
	Dmtu	532 ± 9	48 ± 2	−46 ± 6
	Tmtu	351 ± 4	38 ± 1	−93 ± 4
3				
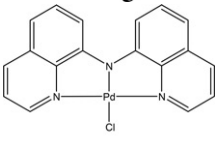	Tu	181 ± 3	42 ± 1	−57 ± 2
	Dmtu	100 ± 2	38 ± 1	−73 ± 3
	Tmtu	74 ± 10	37 ± 2	−76 ± 6
4				

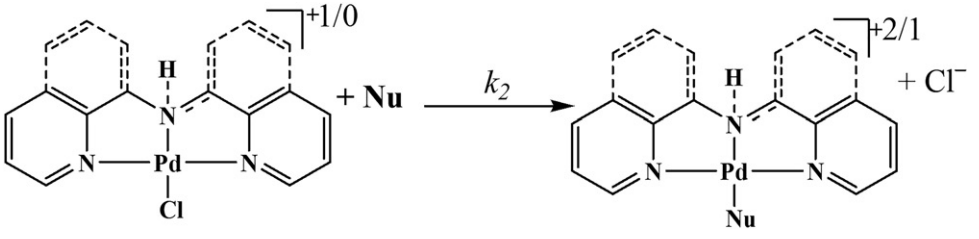

Scheme 2. Proposed reaction mechanism.

$$\ln\left(\frac{k_2}{T}\right) = -\frac{\Delta H^{\neq}}{RT} + \left(23.8 + \frac{\Delta S^{\neq}}{R}\right), \quad (2)$$

where T and R represent temperature and gas constant, respectively. Representative Eyring plots for the reactions of **4** are presented in Figure 3; similar plots for the reactions of other complexes are shown in Figures S19–S21 while the values of $\frac{1}{T}$ with their respective $\ln\left(\frac{k_2}{T}\right)$ are summarized in Tables S6–S9 in the Supporting Information (ESI‡). In addition, the calculated activation parameter values are summarized in Table 3.

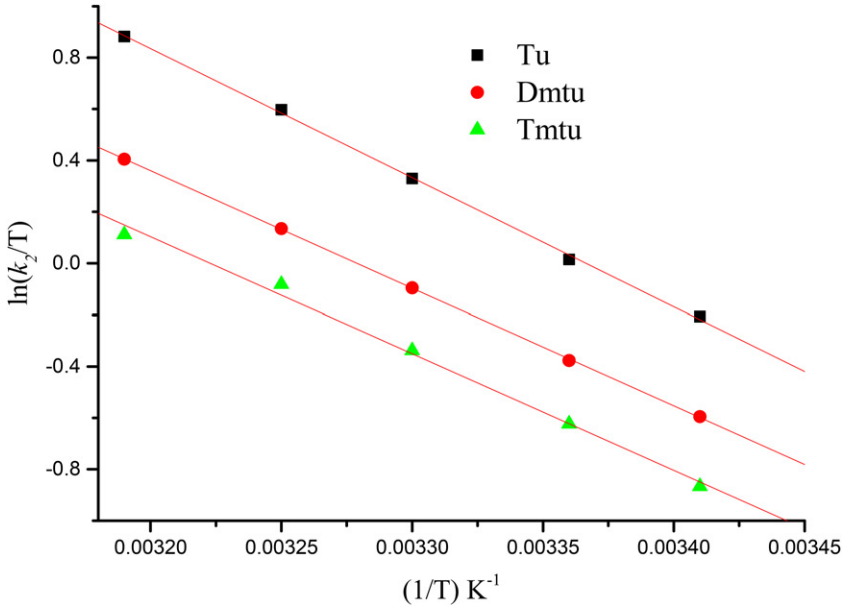

Figure 3. Eyring plots the reactions of **4** with thiourea nucleophiles at different temperatures.

4. Discussion

The reactivity of Pd(II) complexes with varied degrees of π-conjugation was investigated by carefully replacing 2-pyridylmethyl groups of the bis(2-pyridylmethyl)amine (bpma) ligand in **1** with 8-quinolinyl groups resulting in the other complexes. The quinolinyl moiety, known to have both π-acceptor/donor phenyl and an electron deficient pyridine ring [60], would offer π-extension as well as σ-donation. The intention was to try to understand how the competing effect of the net σ-donation of the quinolinyl moiety and the increasing π-conjugation of the complexes will control the reactivity of Pd(II).

In **2**, one of the 2-pyridylmethyl groups in bpma of **1** is replaced by 8-quinolinyl group while both rings are replaced in **4**. In **3**, an imine bond replaces amino methyl bond in the ligand of **2**. In doing so, the substitution rate of the labile chloride ligand from the complexes decreased in the order **1** > **3** > **2** > **4** for all the nucleophiles. All the measured rate constants and activation parameters ($\Delta H^{\#}$ and $\Delta S^{\#}$) are given in Table 3. The reactivity trend observed in the Pd(II) complexes can be explained in terms of the electronic effects caused by the quinolinyl moiety in the ligand framework.

Quinoline having a net σ-donor effect is expected to be less acidic than pyridine since more resonance structures can be drawn to delocalize the positive charge on the conjugate acid [61]. Furthermore, inductive effects of quinoline also play a role in stabilizing the conjugate acid. The less acidic nature of the quinoline ligand in a complex implies an increase in σ-inductive effects in the complex which reduces the ligand's π-acceptability. Quinoline forms several charge transfer complexes by acting as a good σ-donor [62]. This effect usually leads to destabilization of the 18-electron five-coordinate intermediate thereby reducing the reactivity.

The second-order rate constants in Table 3 show that replacing one of the 2-pyridinylmethyl groups of the bpma ligand in **1** with 8-quinolylinyl moiety increases π-conjugation of the ligand of **2** but reduces its reactivity by factors of between 5 and 7 relative to **1** depending on the steric bulk of the incoming nucleophiles. This is similar to what has been reported [22] in $[Pt(terpy)Cl]^+$ complexes when a replacement of one of the *cis*-positioned pyridine rings of terpyridine ligand with an isoquinoline caused an unusual reduction in the rate of substitution by a factor of 4 with the same nucleophiles. The high reactivity of **1** is because of its isolated pyridine rings which are strong π-acceptors withdrawing electron density from Pd(II) through π-backbonding. This makes it more electrophilic as a result of electron density delocalization [20, 24] than **2** and hence more susceptible to nucleophilic attack [30, 32, 63]. The 8-quinolinyl moiety weakens the π-acceptability of the resultant ligand in **2** through σ-inductive effects as well as donating electrons towards the metal center. This increases the electron density around the metal, making it less electrophilic, and retards the swift attack of the incoming nucleophiles as already reported when quinolinyl or isoquinolinyl formed part of the *cis*-spectator tridentate ligand [18, 22, 36, 64]. This is supported by the calculated electrophilicity indices in Table 3 where **2** (5.696) has lower values than **1** (6.077).

When the reactivities of **2** and **4** are compared with that of **3**, **3** is faster by factors of 1 and 5, for all the nucleophiles, in relation to that of **2** and **4**, respectively. The ligand of **2** is bridged by an imine to confer extended π-conjugation and hence enhanced electron delocalization of the ligand in **3** compared to **2**. Indeed, this improves the π-acceptor property of the entire imine-bridged ligand, making it more electrophilic than the complexes and hence a higher rate of substitution. Because of the σ-donor properties of the 8-quinolinyl group, the acceleration of the rate is not as expected based on its extended π-surface. It is well known that Pt(II) complexes of N∘N∘N tridentate ligands with π-conjugated molecular orbitals show high rates of substitution [6, 9, 19, 21, 22, 27, 29]. The reactivity of **4** is lower than those of **2** and **3** because of the σ-donor effects of the two 8-quinolinyl groups retarding its reactivity in comparison to other complexes.

However, the deceleration of the incoming nucleophiles in the substitution process is further observed by factors ranging between 25 and 30 times relative to that of **1** when its bpma ligand is replaced with bis(8-quinolinyl)amine ligand in **4**. This further confirms the fact that the 8-quinolinyl moiety, just like its cousin isoquinolinyl, is a poor π-acceptor of electron density from the metal-based orbitals, while it donates towards the metal center through the lateral bonds. This makes quinoline-based ligand better in stabilizing the metal center than the pyridine-based ligand. The electrophilicity of the metal is thus lowered leading to reduced rate of substitution. Interestingly, through the π-resonance at the amido group, the ligand of **4** has the highest π-surface yet it is the most inert towards substitution. Unlike in **3** whose acceleration in reactivity is due to extended π-surface, though not as expected, the reactivity of **4** is contrary to the expectation that it should be the most reactive. It has been observed that the bis(8-quinolinyl)amine ligand in **4** is monoanionic when coordinated to a metal, as opposed to similar donor ligands such as terpy and its derivatives, leading to its complex being more electron-rich than those of terpy complexes [65].

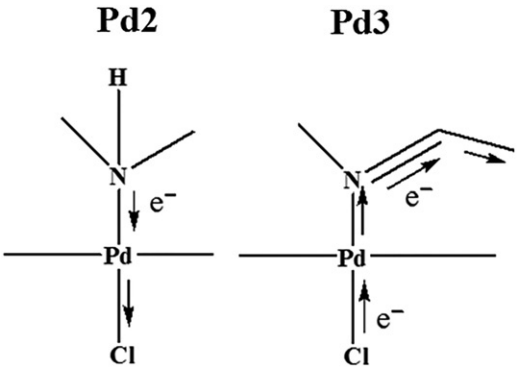

Figure 4. A pictorial illustration of the nature of change in the *trans*-effect indicating flow of electron density in **2** and **3**.

Therefore, the lower reactivity of **4** than the rest of the complexes, despite its large π-surface, is due to the electron-rich environment caused by the good σ-donation, larger σ-inductive effects as well as poor π-acceptability of the quinolinyl moiety. This results in repulsion of the incoming nucleophiles, dampening of the reactivity [40]. This is supported by the smaller NBO charges and electrophilicity index than the other complexes. In addition, the LUMO energy in **4** is also higher, confirming that it is the harder complex and a poorer electrophile [66].

From the DFT calculations, the electrophilicity indices of the complexes decreasing from **1** to **4** with exception of **3** supports the general reactivity trend. The electrophilicity of **3** is out of place because of the change in the nature of the *trans*-effect [9]. For example, in **2** the *trans*-effect is characterized with σ-donation from the amine into the *trans* axis of the complex while in **3** the strong π-acceptor character introduced by imine acts by draining electron density from the metal and the *trans*- chloride orbitals as depicted in Figure 4. The interactions between the d_z^2-orbitals of the metal and the ligand's p_z-orbitals are thus increased in **3** leading to shortening of the Pd–Cl bond as well as making Pd, N2 and Cl centers more positive than those of **2** as depicted in their NBO charges in Table 2. However, the moderate difference in the reactivity between **3** and **2**, despite the large electrophilicity index difference, is an indication that the net σ-donor effect of the ligand moiety (which is larger in **3** than **2**) is still powerful and prevails upon their reactivity.

The trend in the HOMO-LUMO energy difference decreasing from **1** going to **4** reflects the increasing trend of π-conjugation as depicted in Table 2, indicating that the reactivity should increase in that order [66]. However, this notion is counteracted by the dipole moment and the electrophilicity of the majority of the complexes being in good agreement with the reactivity trend. As already shown 8-quinolinyl plays two roles on the complexes, *viz.* enhancing π-extension and σ-donation effects. Based on the results, it is clear that the σ-donation effect is the dominant effect that controls the reactivity of the complexes over the π-back bonding. This explains why the resultant reactivity trend of the Pd(II) complexes is opposite to the increasing π-conjugation in the investigated systems.

As depicted from Table 3, the reactivity with respect to thiourea nucleophiles decreases in the order Tu > Dmtu > Tmtu in all the complexes. This order agrees with their sizes and steric demands. In addition, the substitution of the chloride from the Pd(II)

complexes by thiourea nucleophiles follows the two-term rate law in accordance with associatively activated mode of mechanism which is common for square planar d^8 complexes [67–69]. This conclusion is in agreement with the values of activation enthalpies ($\Delta H^{\neq}$) being positive and relatively low, while entropies ($\Delta S^{\neq}$) are all negative.

5. Conclusion

This study has shown that the reactivity of Pd can be controlled using quinoline moiety as part of the complex's ligand framework. The reactivity of the Pd was reduced by factors of between 25 and 30 for the studied nucleophiles when the bis(2-pyridylmethyl)amine ligand of **1** (strong π-acceptors) was replaced by bis(8-quinolinyl)amine in **4** (good σ-donors). It is evident that the σ-donation and inductive effects of 8-quinolinyl moiety weakens the π-back donation effect of the entire ligand framework, making the metal center less electrophilic and less reactive. This means that comparing π-back bonding in systems of this nature, the σ-effect has more dominant effect in controlling the reactivity, slowing it when not in *trans* and accelerating it when in *trans* as shown in the literature [21, 25]. The mode of mechanism remains associative in nature.

Acknowledgments

We remain grateful to the University of KwaZulu-Natal for financial support and bursary awarded to Daniel Onunga. The authors are equally thankful to C. Grimmer for NMR analysis and C. Janse van Rensburg for elemental and MS analyses.

Disclosure statement

No potential conflict of interest was reported by the authors.

Funding

This work was supported by the University of KwaZulu-Natal, South Africa.

ORCID

Deogratius Jaganyi http://orcid.org/0000-0003-4499-6877

References

[1] J. Bogojeski, R. Jelić, D. Petrović, E. Herdtweck, P.G. Jones, M. Tamm, Ž.D. Bugarčić. *Dalton Trans.*, **40**, 6515 (2011).
[2] E. Breet, R. Van Eldik. *Inorg. Chem.*, **23**, 1865 (1984).
[3] Ž.D. Bugarčić, J. Bogojeski, B. Petrović, S. Hochreuther, R. van Eldik. *Dalton Trans.*, **41**, 12329 (2012).
[4] Ž.D. Bugarčić, J. Bogojeski, R. van Eldik. *Coord. Chem. Rev.*, **292**, 91 (2015).
[5] M. Chipangura, A. Mambanda, D. Jaganyi. *J. Coord. Chem.*, **67**, 2048 (2014).

[6] B. Petrović, Z.D. Bugarčić, A. Dees, I. Ivanović-Burmazović, F.W. Heinemann, R. Puchta, S.N. Steinmann, C. Corminboeuf, R. Van Eldik. *Inorg. Chem.*, **51**, 1516 (2012).
[7] Ž.D. Bugarčić, D.M. Jančić, A.A. Shoukry, M.M. Shoukry. *Monatsh. Chem.*, **135**, 151 (2004).
[8] P. Illner, S. Kern, S. Begel, R. van Eldik. *Chem. Commun.*, 4803 (2007).
[9] M. Đurović, J. Bogojeski, B. Petrović, D. Petrović, F.W. Heinemann, Ž.D. Bugarčić. *Polyhedron*, **41**, 70 (2012).
[10] M. Marques. *ISRN Spectroscopy*, **2013**, 1 (2013).
[11] A.S. Abu-Surrah, M. Kettunen. *Curr. Med. Chem.*, **13**, 1337 (2006).
[12] A. Mijatović, J. Bogojeski, B. Petrović, Ž.D. Bugarčić. *Inorg. Chim. Acta*, **383**, 300 (2012).
[13] B. Rosenberg, L. Vancamp, J.E. Trosko, V.H. Mansour. *Nature*, **222**, 385 (1969).
[14] B. Lippert, *Cisplatin: Chemistry and Biochemistry of a Leading Anticancer Drug*, p. 73, John Wiley & Sons, Zürich, Switzerland (1999).
[15] Ž.D. Bugarčič, G. Liehr, R. van Eldik. *J. Chem. Soc., Dalton Trans.*, **0**, 2825 (2002).
[16] M.D. Hall, M. Okabe, D.-W. Shen, X.-J. Liang, M.M. Gottesman. *Annu. Rev. Pharmacol. Toxicol.*, **48**, 495 (2008).
[17] A.S. Abu-Surrah, H.H. Al-Sa'doni, M.Y. Abdalla. *Cancer Ther.*, **6**, 1 (2008).
[18] I.M. Wekesa, D. Jaganyi. *Dalton Trans.*, **43**, 2549 (2014).
[19] D. Reddy, K.J. Akerman, M.P. Akerman, D. Jaganyi. *Transition Met. Chem.*, **36**, 593 (2011).
[20] D. Jaganyi, A. Hofmann, R. van Eldik. *Angew. Chem. Int. Ed. Engl.*, **40**, 1680 (2001).
[21] D. Jaganyi, D. Reddy, J. Gertenbach, A. Hofmann, R. van Eldik. *Dalton Trans.*, 299 (2004).
[22] P. Ongoma, D. Jaganyi. *Dalton Trans.*, **41**, 10724 (2012).
[23] D. Jaganyi, F. Tiba, O.Q. Munro, B. Petrović, Ž.D. Bugarčić. *Dalton Trans.*, 2943 (2006).
[24] A. Hofmann, D. Jaganyi, O.Q. Munro, G. Liehr, R. van Eldik. *Inorg. Chem.*, **42**, 1688 (2003).
[25] A. Hofmann, L. Dahlenburg, R. van Eldik. *Inorg. Chem.*, **42**, 6528 (2003).
[26] A. Mambanda, D. Jaganyi. In *Advances in Inorganic Chemistry*, Vol. **70**, pp. 243–276, Elsevier, Inc., Burlington (2017).
[27] I.M. Wekesa, D. Jaganyi. *J. Coord. Chem.*, **69**, 389 (2016).
[28] A. Mambanda, D. Jaganyi. *Dalton Trans.*, **40**, 79 (2011).
[29] D. Jaganyi, K.L.D. Boer, J. Gertenbach, J. Perils. *Int. J. Chem. Kinet.*, **40**, 808 (2008).
[30] Ž.D. Bugarčić, G. Liehr, R. van Eldik. *J. Chem. Soc., Dalton Trans.*, 951 (2002).
[31] S. Kern, P. Illner, S. Begel, R. van Eldik. *Eur. J. Inorg. Chem.*, **2010**, 4658 (2010).
[32] D. Jaganyi, F. Tiba. *Transition Met. Chem.*, **28**, 803 (2003).
[33] B. Pitteri, G. Marangoni, L. Cattalini, F. Visentin, V. Bertolasi, P. Gilli. *Polyhedron*, **20**, 869 (2001).
[34] J. Bogojeski, Ž.D. Bugarčić. *Transition Met. Chem.*, **36**, 73 (2011).
[35] A. Shaira, Heterometallic Ruthenium(II)-Platinum(II) Complexes – A New Paradigm A Kinetic, Mechanistic and Computational Investigation into Substitution Behaviour. PhD thesis, University of KwaZulu-Natal (2013).
[36] B.B. Khusi, A. Mambanda, D. Jaganyi. *J. Coord. Chem.*, **69**, 2121 (2016).
[37] H. Zorbas, B.K. Keppler. *ChemBioChem.*, **6**, 1157 (2005).
[38] S. van Zutphen, J. Reedijk. *Coord. Chem. Rev.*, **249**, 2845 (2005).
[39] N.P. Barry, P.J. Sadler. *Chem. Commun. (Camb.)* **49**, 5106 (2013).
[40] G. Kinunda, D. Jaganyi. *Transition Met. Chem.*, **39**, 451 (2014).
[41] L. Carlsen, H. Egsgaard, J.R. Andersen. *Anal. Chem.*, **51**, 1593 (1979).
[42] J. Lu, Q. Sun, J.-L. Li, W. Gu, J.-L. Tian, X. Liu, S.-P. Yan. *J. Coord. Chem.*, **66**, 3280 (2013).
[43] J.C. Peters, S.B. Harkins, S.D. Brown, M.W. Day. *Inorg. Chem.*, **40**, 5083 (2001).
[44] B.A. Kruis, J. Boersma. *Organometallics*, **14**, 4213 (1995).
[45] C.F. Weber, R. van Eldik. *Eur. J. Inorg. Chem.*, **2005**, 4755 (2005).
[46] M. Bortoluzzi, G. Paolucci, B. Pitteri, P. Zennaro, V. Bertolasi. *J. Organomet. Chem.*, **696**, 2565 (2011).
[47] M. Bortoluzzi, G. Paolucci, B. Pitteri, A. Vavasori. *Inorg. Chem. Commun.*, **9**, 1301 (2006).
[48] M. Kosović, Ž. Jaćimović, Ž.D. Bugarčić, B.V. Petrović. *Transition Met. Chem.*, **41**, 161 (2016).
[49] S. Jovanović, B. Petrović, D. Čanović, Ž.D. Bugarčić. *Int. J. Chem. Kinet.*, **43**, 99 (2011).

[50] M. Tobe, J. Burgess, *Inorganic Reaction Mechanisms*, pp. 30–39, Addison Wesley Longman Inc., Essex (1999).
[51] M. Frisch, G. Trucks, H. Schlegel, G. Scuseria, M. Robb, J. Cheeseman, G. Scalmani, V. Barone, B. Mennucci, G. Petersson, *Gaussian 09, revision D. 01*, Gaussian, Inc., Wallingford, CT (2009).
[52] P.J. Hay, W.R. Wadt. *J. Chem. Phys.*, **82**, 299 (1985).
[53] V. Barone, M. Cossi. *J. Phys. Chem. A*, **102**, 1995 (1998).
[54] M. Cossi, N. Rega, G. Scalmani, V. Barone. *J. Comput. Chem.*, **24**, 669 (2003).
[55] S.B. Harkins, J.C. Peters. *Organometallics*, **21**, 1753 (2002).
[56] C.A. Mebi. *J. Chem. Sci.*, **123**, 727 (2011).
[57] R.G. Parr, L. v. Szentpály, S. Liu. *J. Am. Chem. Soc.*, **121**, 1922 (1999).
[58] OriginPro 9.1. OriginLab Corporation, One Roundhouse Plaza, Suite 303, Northampton, MA 01060, United States. 1800-969-7720
[59] H. Eyring. *J. Chem. Phys.*, **3**, 107 (1935).
[60] P. Bruice, *Organic Chemistry*, 2nd edn, Prentice-Hall, Upper Saddle River, NJ (1998).
[61] R.S. Hosmane, J.F. Liebman. *Struct. Chem.*, **20**, 693 (2009).
[62] J. Gurnos, *The Chemistry of Heterocyclic Compounds*. In: *Quinolines*, pp. 9, Wiley, London (2009).
[63] Ž.D. Bugarčić, B. Petrović, E. Zangrando. *Inorg. Chim. Acta*, **357**, 2650 (2004).
[64] A. Shaira, D. Reddy, D. Jaganyi. *Dalton Trans.*, **42**, 8426 (2013).
[65] T.A. Betley, B.A. Qian, J.C. Peters. *Inorg. Chem.*, **47**, 11570 (2008).
[66] R. Singh, K. Suresh, D. Prabhu. *Int. J. Chemtech. Res.*, **3**, 1571 (2011).
[67] F. Basolo, R.G. Pearson, *Mechanisms in Inorganic Reactions*, 2nd edn, pp. 193–198, Wiley, New York (1967).
[68] J.D. Atwood, *Inorganic and Organometallic Reaction Mechanisms*, 2nd edn, p. 63, Wiley-VCH Publishers, New York (1997).
[69] R. Van Eldik, T. Asano, W. Le Noble. *Chem. Rev.*, **89**, 549 (1989).